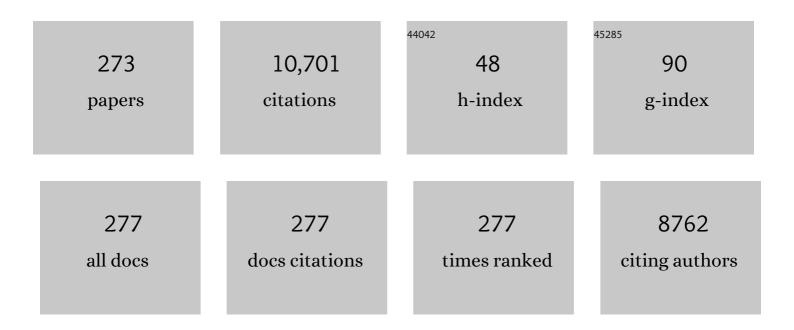
## Onisimo Mutanga

List of Publications by Year in descending order

Source: https://exaly.com/author-pdf/5917073/publications.pdf Version: 2024-02-01



#	Article	IF	CITATIONS
1	Multispectral and hyperspectral remote sensing for identification and mapping of wetland vegetation: a review. Wetlands Ecology and Management, 2010, 18, 281-296.	0.7	723
2	High density biomass estimation for wetland vegetation using WorldView-2 imagery and random forest regression algorithm. International Journal of Applied Earth Observation and Geoinformation, 2012, 18, 399-406.	1.4	574
3	Narrow band vegetation indices overcome the saturation problem in biomass estimation. International Journal of Remote Sensing, 2004, 25, 3999-4014.	1.3	563
4	Google Earth Engine Applications Since Inception: Usage, Trends, and Potential. Remote Sensing, 2018, 10, 1509.	1.8	402
5	Land-use/cover classification in a heterogeneous coastal landscape using RapidEye imagery: evaluating the performance of random forest and support vector machines classifiers. International Journal of Remote Sensing, 2014, 35, 3440-3458.	1.3	304
6	Predicting in situ pasture quality in the Kruger National Park, South Africa, using continuum-removed absorption features. Remote Sensing of Environment, 2004, 89, 393-408.	4.6	263
7	Google Earth Engine Applications. Remote Sensing, 2019, 11, 591.	1.8	262
8	Evaluating the utility of the medium-spatial resolution Landsat 8 multispectral sensor in quantifying aboveground biomass in uMgeni catchment, South Africa. ISPRS Journal of Photogrammetry and Remote Sensing, 2015, 101, 36-46.	4.9	220
9	Red edge shift and biochemical content in grass canopies. ISPRS Journal of Photogrammetry and Remote Sensing, 2007, 62, 34-42.	4.9	197
10	Remote Sensing of Above-Ground Biomass. Remote Sensing, 2017, 9, 935.	1.8	153
11	Integrating imaging spectroscopy and neural networks to map grass quality in the Kruger National Park, South Africa. Remote Sensing of Environment, 2004, 90, 104-115.	4.6	136
12	Forage quality of savannas — Simultaneously mapping foliar protein and polyphenols for trees and grass using hyperspectral imagery. Remote Sensing of Environment, 2010, 114, 64-72.	4.6	134
13	Detecting Sirex noctilio grey-attacked and lightning-struck pine trees using airborne hyperspectral data, random forest and support vector machines classifiers. ISPRS Journal of Photogrammetry and Remote Sensing, 2014, 88, 48-59.	4.9	132
14	Spectral discrimination of papyrus vegetation (Cyperus papyrus L.) in swamp wetlands using field spectrometry. ISPRS Journal of Photogrammetry and Remote Sensing, 2009, 64, 612-620.	4.9	131
15	Examining the potential of Sentinel-2 MSI spectral resolution in quantifying above ground biomass across different fertilizer treatments. ISPRS Journal of Photogrammetry and Remote Sensing, 2015, 110, 55-65.	4.9	128
16	Hyperspectral band depth analysis for a better estimation of grass biomass (Cenchrus ciliaris) measured under controlled laboratory conditions. International Journal of Applied Earth Observation and Geoinformation, 2004, 5, 87-96.	1.4	121
17	Discriminating tropical grass (Cenchrus ciliaris) canopies grown under different nitrogen treatments using spectroradiometry. ISPRS Journal of Photogrammetry and Remote Sensing, 2003, 57, 263-272.	4.9	113
18	Investigating the robustness of the new Landsat-8 Operational Land Imager derived texture metrics in estimating plantation forest aboveground biomass in resource constrained areas. ISPRS Journal of Photogrammetry and Remote Sensing, 2015, 108, 12-32.	4.9	112

#	Article	IF	CITATIONS
19	Commercial tree species discrimination using airborne AISA Eagle hyperspectral imagery and partial least squares discriminant analysis (PLS-DA) in KwaZulu–Natal, South Africa. ISPRS Journal of Photogrammetry and Remote Sensing, 2013, 79, 19-28.	4.9	109
20	Intra-and-Inter Species Biomass Prediction in a Plantation Forest: Testing the Utility of High Spatial Resolution Spaceborne Multispectral RapidEye Sensor and Advanced Machine Learning Algorithms. Sensors, 2014, 14, 15348-15370.	2.1	105
21	Estimating tropical pasture quality at canopy level using band depth analysis with continuum removal in the visible domain. International Journal of Remote Sensing, 2005, 26, 1093-1108.	1.3	103
22	Examining the strength of the newly-launched Sentinel 2 MSI sensor in detecting and discriminating subtle differences between C3 and C4 grass species. ISPRS Journal of Photogrammetry and Remote Sensing, 2017, 129, 32-40.	4.9	102
23	Nitrogen detection with hyperspectral normalized ratio indices across multiple plant species. International Journal of Remote Sensing, 2005, 26, 4083-4095.	1.3	101
24	A comparison of regression tree ensembles: Predicting Sirex noctilio induced water stress in Pinus patula forests of KwaZulu-Natal, South Africa. International Journal of Applied Earth Observation and Geoinformation, 2010, 12, S45-S51.	1.4	98
25	Estimating standing biomass in papyrus ( <i>Cyperus papyrus</i> L.) swamp: exploratory of <i>in situ</i> hyperspectral indices and random forest regression. International Journal of Remote Sensing, 2014, 35, 693-714.	1.3	91
26	Discriminating the papyrus vegetation ( <i>Cyperus papyrus</i> L) and its co-existent species using random forest and hyperspectral data resampled to HYMAP. International Journal of Remote Sensing, 2012, 33, 552-569.	1.3	89
27	Evaluating the impact of red-edge band from Rapideye image for classifying insect defoliation levels. ISPRS Journal of Photogrammetry and Remote Sensing, 2014, 95, 34-41.	4.9	86
28	Exploiting machine learning algorithms for tree species classification in a semiarid woodland using RapidEye image. Journal of Applied Remote Sensing, 2013, 7, 073480.	0.6	75
29	Performance of Support Vector Machines and Artificial Neural Network for Mapping Endangered Tree Species Using WorldView-2 Data in Dukuduku Forest, South Africa. IEEE Journal of Selected Topics in Applied Earth Observations and Remote Sensing, 2015, 8, 4825-4840.	2.3	72
30	Discriminating indicator grass species for rangeland degradation assessment using hyperspectral data resampled to AISA Eagle resolution. ISPRS Journal of Photogrammetry and Remote Sensing, 2012, 70, 56-65.	4.9	71
31	Separability of coffee leaf rust infection levels with machine learning methods at Sentinel-2 MSI spectral resolutions. Precision Agriculture, 2017, 18, 859-881.	3.1	71
32	Random Forests Unsupervised Classification: The Detection and Mapping of <i>Solanum mauritianum</i> Infestations in Plantation Forestry Using Hyperspectral Data. IEEE Journal of Selected Topics in Applied Earth Observations and Remote Sensing, 2015, 8, 3107-3122.	2.3	68
33	Prediction of future urban surface temperatures using medium resolution satellite data in Harare metropolitan city, Zimbabwe. Building and Environment, 2017, 122, 397-410.	3.0	68
34	A comparison of partial least squares (PLS) and sparse PLS regressions for predicting yield of Swiss chard grown under different irrigation water sources using hyperspectral data. Computers and Electronics in Agriculture, 2014, 106, 11-19.	3.7	67
35	Estimating and mapping grass phosphorus concentration in an African savanna using hyperspectral image data. International Journal of Remote Sensing, 2007, 28, 4897-4911.	1.3	64
36	Water quality monitoring in sub-Saharan African lakes: a review of remote sensing applications. African Journal of Aquatic Science, 2015, 40, 1-7.	0.5	64

ΟΝΙΣΙΜΟ Μυτάνδα

#	Article	IF	CITATIONS
37	Remote sensing of species diversity using Landsat 8 spectral variables. ISPRS Journal of Photogrammetry and Remote Sensing, 2017, 133, 116-127.	4.9	62
38	Progress in the remote sensing of C3 and C4 grass species aboveground biomass over time and space. ISPRS Journal of Photogrammetry and Remote Sensing, 2016, 120, 13-24.	4.9	60
39	Multi-phenology WorldView-2 imagery improves remote sensing of savannah tree species. International Journal of Applied Earth Observation and Geoinformation, 2017, 58, 65-73.	1.4	60
40	Advancements in satellite remote sensing for mapping and monitoring of alien invasive plant species (AIPs). Physics and Chemistry of the Earth, 2019, 112, 237-245.	1.2	59
41	Investigating the Capability of Few Strategically Placed Worldview-2 Multispectral Bands to Discriminate Forest Species in KwaZulu-Natal, South Africa. IEEE Journal of Selected Topics in Applied Earth Observations and Remote Sensing, 2014, 7, 307-316.	2.3	55
42	Determining extreme heat vulnerability of Harare Metropolitan City using multispectral remote sensing and socio-economic data. Journal of Spatial Science, 2018, 63, 173-191.	1.0	55
43	Mapping Solanum mauritianum plant invasions using WorldView-2 imagery and unsupervised random forests. Remote Sensing of Environment, 2016, 182, 39-48.	4.6	53
44	Evaluating the robustness of models developed from field spectral data in predicting African grass foliar nitrogen concentration using WorldView-2 image as an independent test dataset. International Journal of Applied Earth Observation and Geoinformation, 2015, 34, 178-187.	1.4	52
45	Using WorldView-2 bands and indices to predict bronze bug (Thaumastocoris peregrinus) damage in plantation forests. International Journal of Remote Sensing, 2013, 34, 2236-2249.	1.3	51
46	Remotely sensed retrieval of Local Climate Zones and their linkages to land surface temperature in Harare metropolitan city, Zimbabwe. Urban Climate, 2019, 27, 259-271.	2.4	51
47	Explaining grassâ€nutrient patterns in a savanna rangeland of southern Africa. Journal of Biogeography, 2004, 31, 819-829.	1.4	50
48	Mapping spatial variability of foliar nitrogen in coffee (Coffea arabica L.) plantations with multispectral Sentinel-2 MSI data. ISPRS Journal of Photogrammetry and Remote Sensing, 2018, 138, 1-11.	4.9	50
49	Linking remotely sensed forage quality estimates from WorldView-2 multispectral data with cattle distribution in a savanna landscape. International Journal of Applied Earth Observation and Geoinformation, 2013, 21, 513-524.	1.4	49
50	Application of remote sensing in estimating maize grain yield in heterogeneous African agricultural landscapes: a review. International Journal of Remote Sensing, 2017, 38, 6816-6845.	1.3	48
51	How to build science-action partnerships for local land-use planning and management: lessons from Durban, South Africa. Ecology and Society, 2016, 21, .	1.0	47
52	Testing the reliability and stability of the internal accuracy assessment of random forest for classifying tree defoliation levels using different validation methods. Geocarto International, 2015, 30, 810-821.	1.7	46
53	Modeling the Potential Distribution of Pine Forests Susceptible to <i>Sirex Noctilio</i> Infestations in GIS, 2010, 14, 709-726.	1.0	45
54	Assessing the potential of integrated Landsat 8 thermal bands, with the traditional reflective bands and derived vegetation indices in classifying urban landscapes. Geocarto International, 2017, 32, 886-899.	1.7	45

#	Article	IF	CITATIONS
55	Estimating Biomass of Native Grass Grown under Complex Management Treatments Using WorldView-3 Spectral Derivatives. Remote Sensing, 2017, 9, 55.	1.8	45
56	Detecting the Early Stage of Phaeosphaeria Leaf Spot Infestations in Maize Crop Using In Situ Hyperspectral Data and Guided Regularized Random Forest Algorithm. Journal of Spectroscopy, 2017, 2017, 1-8.	0.6	45
57	Advancements in the remote sensing of landscape pattern of urban green spaces and vegetation fragmentation. International Journal of Remote Sensing, 2021, 42, 3797-3832.	1.3	45
58	Empirical Prediction of Leaf Area Index (LAI) of Endangered Tree Species in Intact and Fragmented Indigenous Forests Ecosystems Using WorldView-2 Data and Two Robust Machine Learning Algorithms. Remote Sensing, 2016, 8, 324.	1.8	44
59	Linking major shifts in land surface temperatures to long term land use and land cover changes: A case of Harare, Zimbabwe. Urban Climate, 2017, 20, 120-134.	2.4	44
60	Leaf level experiments to discriminate between eucalyptus species using high spectral resolution reflectance data: use of derivatives, ratios and vegetation indices. Geocarto International, 2010, 25, 327-344.	1.7	41
61	Comparing the spectral settings of the new generation broad and narrow band sensors in estimating biomass of native grasses grown under different management practices. GIScience and Remote Sensing, 2016, 53, 614-633.	2.4	41
62	Detection and mapping the spatial distribution of bracken fern weeds using the Landsat 8 OLI new generation sensor. International Journal of Applied Earth Observation and Geoinformation, 2017, 57, 93-103.	1.4	41
63	Application of Drone Technologies in Surface Water Resources Monitoring and Assessment: A Systematic Review of Progress, Challenges, and Opportunities in the Global South. Drones, 2021, 5, 84.	2.7	41
64	Discriminating Sirex noctilio Attack in Pine Forest Plantations in South Africa Using High Spectral Resolution Data. , 2008, , 161-175.		41
65	The utility of Sentinel-2 Vegetation Indices (VIs) and Sentinel-1 Synthetic Aperture Radar (SAR) for invasive alien species detection and mapping. Nature Conservation, 0, 35, 41-61.	0.0	39
66	Integrating remote sensing and spatial statistics to model herbaceous biomass distribution in a tropical savanna. International Journal of Remote Sensing, 2006, 27, 3499-3514.	1.3	38
67	Discriminating the early stages of <i>Sirex noctilio</i> infestation using classification tree ensembles and shortwave infrared bands. International Journal of Remote Sensing, 2011, 32, 4249-4266.	1.3	38
68	Potential utility of the spectral red-edge region of SumbandilaSat imagery for assessing indigenous forest structure and health. International Journal of Applied Earth Observation and Geoinformation, 2012, 16, 85-93.	1.4	38
69	Mapping forest aboveground biomass in the reforested Buffelsdraai landfill site using texture combinations computed from SPOT-6 pan-sharpened imagery. International Journal of Applied Earth Observation and Geoinformation, 2019, 74, 65-77.	1.4	38
70	Predicting <i>Eucalyptus</i> spp. stand volume in Zululand, South Africa: an analysis using a stochastic gradient boosting regression ensemble with multi-source data sets. International Journal of Remote Sensing, 2015, 36, 3751-3772.	1.3	37
71	Land surface temperature and emissivity estimation for Urban Heat Island assessment using medium- and low-resolution space-borne sensors: A review. Geocarto International, 2017, 32, 455-470.	1.7	37
72	Discriminating Rangeland Management Practices Using Simulated HyspIRI, Landsat 8 OLI, Sentinel 2 MSI, and VENµS Spectral Data. IEEE Journal of Selected Topics in Applied Earth Observations and Remote Sensing, 2016, 9, 3957-3969.	2.3	36

#	Article	IF	CITATIONS
73	Predicting Spatial Distribution of Key Honeybee Pests in Kenya Using Remotely Sensed and Bioclimatic Variables: Key Honeybee Pests Distribution Models. ISPRS International Journal of Geo-Information, 2017, 6, 66.	1.4	36
74	A quantitative framework for analysing long term spatial clustering and vegetation fragmentation in an urban landscape using multi-temporal landsat data. International Journal of Applied Earth Observation and Geoinformation, 2020, 88, 102057.	1.4	36
75	Reducing Leaf-Level Hyperspectral Data to 22 Components of Biochemical and Biophysical Bands Optimizes Tree Species Discrimination. IEEE Journal of Selected Topics in Applied Earth Observations and Remote Sensing, 2015, 8, 3161-3171.	2.3	35
76	Challenges and opportunities in the use of remote sensing for C <sub>3</sub> and C <sub>4</sub> grass species discrimination and mapping. African Journal of Range and Forage Science, 2012, 29, 47-61.	0.6	34
77	Spectral resampling based on user-defined inter-band correlation filter: C3 and C4 grass species classification. International Journal of Applied Earth Observation and Geoinformation, 2013, 21, 535-544.	1.4	34
78	Spectral Discrimination of Insect Defoliation Levels in Mopane Woodland Using Hyperspectral Data. IEEE Journal of Selected Topics in Applied Earth Observations and Remote Sensing, 2014, 7, 177-186.	2.3	34
79	UAV-Based Multispectral Phenotyping for Disease Resistance to Accelerate Crop Improvement under Changing Climate Conditions. Remote Sensing, 2020, 12, 2445.	1.8	34
80	Forest health and vitality: the detection and monitoring of Pinus patula trees infected by Sirex noctilio using digital multispectral imagery. Southern Forests, 2007, 69, 39-47.	0.2	33
81	Predicting Thaumastocoris peregrinus damage using narrow band normalized indices and hyperspectral indices using field spectra resampled to the Hyperion sensor. International Journal of Applied Earth Observation and Geoinformation, 2013, 21, 113-121.	1.4	33
82	Exploring the potential of <i>in situ</i> hyperspectral data and multivariate techniques in discriminating different fertilizer treatments in grasslands. Journal of Applied Remote Sensing, 2015, 9, 096033.	0.6	32
83	Assessing and mapping the severity of soil erosion using the 30-m Landsat multispectral satellite data in the former South African homelands of Transkei. Physics and Chemistry of the Earth, 2017, 100, 296-304.	1.2	32
84	Estimating tree species diversity in the savannah using NDVI and woody canopy cover. International Journal of Applied Earth Observation and Geoinformation, 2018, 66, 106-115.	1.4	32
85	The impact of land-use/land cover changes on water balance of the heterogeneous Buzi sub-catchment, Zimbabwe. Remote Sensing Applications: Society and Environment, 2020, 18, 100292.	0.8	32
86	A Comparative Estimation of Maize Leaf Water Content Using Machine Learning Techniques and Unmanned Aerial Vehicle (UAV)-Based Proximal and Remotely Sensed Data. Remote Sensing, 2021, 13, 4091.	1.8	32
87	Comparison between WorldView-2 and SPOT-5 images in mapping the bracken fern using the random forest algorithm. Journal of Applied Remote Sensing, 2014, 8, 083527.	0.6	31
88	Predicting C3 and C4 grass nutrient variability using <i>in situ</i> canopy reflectance and partial least squares regression. International Journal of Remote Sensing, 2015, 36, 1743-1761.	1.3	31
89	Remote sensing leaf water stress in coffee ( Coffea arabica ) using secondary effects of water absorption and random forests. Physics and Chemistry of the Earth, 2017, 100, 317-324.	1.2	31
90	Detecting the severity of maize streak virus infestations in maize crop using in situ hyperspectral data. Transactions of the Royal Society of South Africa, 2018, 73, 8-15.	0.8	31

#	Article	IF	CITATIONS
91	Examining the utility of random forest and AISA Eagle hyperspectral image data to predict <i>Pinus patula</i> age in KwaZulu-Natal, South Africa. Geocarto International, 2011, 26, 275-289.	1.7	30
92	Integrating environmental variables and WorldView-2 image data to improve the prediction and mapping of Thaumastocoris peregrinus (bronze bug) damage in plantation forests. ISPRS Journal of Photogrammetry and Remote Sensing, 2014, 87, 39-46.	4.9	30
93	Feature level image fusion of optical imagery and Synthetic Aperture Radar (SAR) for invasive alien plant species detection and mapping. Remote Sensing Applications: Society and Environment, 2018, 10, 198-208.	0.8	30
94	Estimating LAI and mapping canopy storage capacity for hydrological applications in wattle infested ecosystems using Sentinel-2 MSI derived red edge bands. GIScience and Remote Sensing, 2019, 56, 68-86.	2.4	30
95	Testing the capabilities of the new WorldView-3 space-borne sensor's red-edge spectral band in discriminating and mapping complex grassland management treatments. International Journal of Remote Sensing, 2017, 38, 1-22.	1.3	29
96	Deep learning-based national scale soil organic carbon mapping with Sentinel-3 data. Geoderma, 2022, 411, 115695.	2.3	29
97	Towards a framework for measuring end to end performance of land administration business processes $\hat{a} \in A$ case study. Computers, Environment and Urban Systems, 2009, 33, 293-301.	3.3	28
98	Remote sensing of crop health for food security in Africa: Potentials and constraints. Remote Sensing Applications: Society and Environment, 2017, 8, 231-239.	0.8	28
99	Empirical Modeling of Leaf Chlorophyll Content in Coffee (Coffea Arabica) Plantations With Sentinel-2 MSI Data: Effects of Spectral Settings, Spatial Resolution, and Crop Canopy Cover. IEEE Journal of Selected Topics in Applied Earth Observations and Remote Sensing, 2017, 10, 5541-5550.	2.3	28
100	UAV-based high-throughput phenotyping to increase prediction and selection accuracy in maize varieties under artificial MSV inoculation. Computers and Electronics in Agriculture, 2021, 184, 106128.	3.7	28
101	Assessing the effects of subtropical forest fragmentation on leaf nitrogen distribution using remote sensing data. Landscape Ecology, 2013, 28, 1479-1491.	1.9	27
102	Progress in remote sensing: vegetation monitoring in South Africa. Southern African Geographical Journal, 2016, 98, 461-471.	0.9	27
103	Multispectral remote sensing for mapping grassland degradation using the key indicators of grass species and edaphic factors. Geocarto International, 2016, 31, 477-491.	1.7	27
104	Machine learning prediction of coffee rust severity on leaves using spectroradiometer data. Tropical Plant Pathology, 2018, 43, 117-127.	0.8	27
105	Estimating the road edge effect on adjacent <i>Eucalyptus grandis</i> forests in KwaZulu-Natal, South Africa, using texture measures and an artificial neural network. Journal of Spatial Science, 2012, 57, 153-173.	1.0	26
106	Optimizing spectral resolutions for the classification of C3 and C4 grass species, using wavelengths of known absorption features. Journal of Applied Remote Sensing, 2012, 6, 063560-1.	0.6	26
107	Comparison of partial least squares and support vector regressions for predicting leaf area index on a tropical grassland using hyperspectral data. Journal of Applied Remote Sensing, 2016, 10, 036015.	0.6	26
108	Optimising the spatial resolution of WorldView-2 pan-sharpened imagery for predicting levels of Gonipterus scutellatus defoliation in KwaZulu-Natal, South Africa. ISPRS Journal of Photogrammetry and Remote Sensing, 2016, 112, 13-22.	4.9	26

#	Article	IF	CITATIONS
109	Estimating Swiss chard foliar macro- and micronutrient concentrations under different irrigation water sources using ground-based hyperspectral data and four partial least squares (PLS)-based (PLS1,) Tj ETQq1 21-33.	1,0,78431 3.7	l4.rgBT /Ove
110	Testing the capability of spectral resolution of the new multispectral sensors on detecting the severity of grey leaf spot disease in maize crop. Geocarto International, 2018, 33, 1223-1236.	1.7	26
111	Predicting soil organic carbon stocks under commercial forest plantations in KwaZulu-Natal province, South Africa using remotely sensed data. GIScience and Remote Sensing, 2020, 57, 450-463.	2.4	26
112	Estimation of Canopy Nitrogen Concentration Across C3 and C4 Grasslands Using WorldView-2 Multispectral Data. IEEE Journal of Selected Topics in Applied Earth Observations and Remote Sensing, 2014, 7, 4385-4392.	2.3	25
113	Mapping canopy gaps in an indigenous subtropical coastal forest using high-resolution WorldView-2 data. International Journal of Remote Sensing, 2014, 35, 6397-6417.	1.3	25
114	Mapping the occurrence of Chromolaena odorata (L.) in subtropical forest gaps using environmental and remote sensing data. Biological Invasions, 2015, 17, 2027-2042.	1.2	25
115	Detecting bugweed (Solanum mauritianum) abundance in plantation forestry using multisource remote sensing. ISPRS Journal of Photogrammetry and Remote Sensing, 2016, 121, 167-176.	4.9	25
116	Multi-season RapidEye imagery improves the classification of wetland and dryland communities in a subtropical coastal region. ISPRS Journal of Photogrammetry and Remote Sensing, 2019, 157, 171-187.	4.9	25
117	Examining the effectiveness of Sentinel-1 and 2 imagery for commercial forest species mapping. Geocarto International, 2021, 36, 1-12.	1.7	25
118	Combining spectral and textural remote sensing variables using random forests: predicting the age of <i>Pinus patula</i> forests in KwaZulu-Natal, South Africa. Journal of Spatial Science, 2012, 57, 193-211.	1.0	24
119	Feature Selection on Sentinel-2 Multispectral Imagery for Mapping a Landscape Infested by Parthenium Weed. Remote Sensing, 2019, 11, 1892.	1.8	24
120	The identification and remote detection of alien invasive plants in commercial forests: An Overview. South African Journal of Geomatics, 2016, 5, 49.	0.1	23
121	Understanding the relationship between urban outdoor temperatures and indoor air-conditioning energy demand in Zimbabwe. Sustainable Cities and Society, 2017, 34, 97-108.	5.1	23
122	Predicting the spatial suitability distribution of Moringa oleifera cultivation using analytical hierarchical process modelling. South African Journal of Botany, 2020, 129, 161-168.	1.2	23
123	Effect of landscape pattern and spatial configuration of vegetation patches on urban warming and cooling in Harare metropolitan city, Zimbabwe. GIScience and Remote Sensing, 2021, 58, 261-280.	2.4	23
124	DETERMINING THE OPTIMAL SPATIAL RESOLUTION OF REMOTELY SENSED DATA FOR THE DETECTION OF <i>SIREX NOCTILIO</i> INFESTATIONS IN PINE PLANTATIONS IN KWAZULU-NATAL, SOUTH AFRICA. Southern African Geographical Journal, 2008, 90, 22-31.	0.9	22
125	The impact of integrating WorldView-2 sensor and environmental variables in estimating plantation forest species aboveground biomass and carbon stocks in uMgeni Catchment, South Africa. ISPRS Journal of Photogrammetry and Remote Sensing, 2016, 119, 415-425.	4.9	22
126	Remotely sensed C3 and C4 grass species aboveground biomass variability in response to seasonal climate and topography. African Journal of Ecology, 2019, 57, 477-489.	0.4	22

#	Article	IF	CITATIONS
127	Exploring the spatial patterns of vegetation fragmentation using local spatial autocorrelation indices. Journal of Applied Remote Sensing, 2019, 13, 1.	0.6	22
128	Mapping alien and indigenous vegetation in the KwaZulu-Natal Sandstone Sourveld using remotely sensed data. Bothalia, 2016, 46, .	0.2	22
129	Does simultaneous variable selection and dimension reduction improve the classification of <i>Pinus </i> forest species?. Journal of Applied Remote Sensing, 2014, 8, 085194.	0.6	21
130	Quantifying the variability and allocation patterns of aboveground carbon stocks across plantation forest types, structural attributes and age in sub-tropical coastal region of KwaZulu Natal, South Africa using remote sensing. Applied Geography, 2015, 64, 55-65.	1.7	21
131	Testing the detection and discrimination potential of the new LandsatÂ8 satellite data on the challenging water hyacinth ( EichhorniaÂcrassipes ) in freshwater ecosystems. Applied Geography, 2017, 84, 11-22.	1.7	21
132	Estimating forest standing biomass in savanna woodlands as an indicator of forest productivity using the new generation WorldView-2 sensor. Geocarto International, 2018, 33, 178-188.	1.7	21
133	Estimating and Monitoring Land Surface Phenology in Rangelands: A Review of Progress and Challenges. Remote Sensing, 2021, 13, 2060.	1.8	21
134	Predicting plant water content in Eucalyptus grandis forest stands in KwaZulu-Natal, South Africa using field spectra resampled to the Sumbandila Satellite Sensor. International Journal of Applied Earth Observation and Geoinformation, 2010, 12, 158-164.	1.4	20
135	Application of topo-edaphic factors and remotely sensed vegetation indices to enhance biomass estimation in a heterogeneous landscape in the Eastern Arc Mountains of Tanzania. Geocarto International, 2016, 31, 1-21.	1.7	20
136	Developing detailed age-specific thematic maps for coffee ( <i>Coffea arabica</i> L.) in heterogeneous agricultural landscapes using random forests applied on Landsat 8 multispectral sensor. Geocarto International, 2017, 32, 759-776.	1.7	20
137	Quantitative assessment of grassland foliar moisture parameters as an inference on rangeland condition in the mesic rangelands of southern Africa. International Journal of Remote Sensing, 2021, 42, 1474-1491.	1.3	20
138	Seasonal discrimination of C3 and C4 grasses functional types: An evaluation of the prospects of varying spectral configurations of new generation sensors. International Journal of Applied Earth Observation and Geoinformation, 2017, 62, 47-55.	1.4	19
139	Integrating age in the detection and mapping of incongruous patches in coffee (Coffea arabica) plantations using multi-temporal Landsat 8 NDVI anomalies. International Journal of Applied Earth Observation and Geoinformation, 2017, 57, 1-13.	1.4	19
140	Remote sensing applications in monitoring urban growth impacts on in-and-out door thermal conditions: A review. Remote Sensing Applications: Society and Environment, 2017, 8, 83-93.	0.8	19
141	Evaluating the potential of the red edge channel for C3 (Festuca spp.) grass discrimination using Sentinel-2 and Rapid Eye satellite image data. Geocarto International, 2019, 34, 1123-1143.	1.7	19
142	Evaluating the performance of the newly-launched Landsat 8 sensor in detecting and mapping the spatial configuration of water hyacinth ( Eichhornia crassipes ) in inland lakes, Zimbabwe. Physics and Chemistry of the Earth, 2017, 100, 101-111.	1.2	18
143	Mapping leaf nitrogen and carbon concentrations of intact and fragmented indigenous forest ecosystems using empirical modeling techniques and WorldView-2 data. ISPRS Journal of Photogrammetry and Remote Sensing, 2017, 131, 26-39.	4.9	18
144	Detection and mapping of bracken fern weeds using multispectral remotely sensed data: a review of progress and challenges. Geocarto International, 2018, 33, 209-224.	1.7	18

**ONISIMO MUTANGA** 

#	Article	IF	CITATIONS
145	Discriminating sodium concentration in a mixed grass species environment of the Kruger National Park using field spectrometry. International Journal of Remote Sensing, 2004, 25, 4191-4201.	1.3	17
146	Determining the susceptibility ofEucalyptus nitensforests toCoryphodema tristis(cossid moth) occurrence in Mpumalanga, South Africa. International Journal of Geographical Information Science, 2013, 27, 1924-1938.	2.2	17
147	Understanding the spatial distribution of elephant (Loxodonta africana) poaching incidences in the mid-Zambezi Valley, Zimbabwe using Geographic Information Systems and remote sensing. Geocarto International, 2016, 31, 1006-1018.	1.7	17
148	Determination of urban land-cover types and their implication on thermal characteristics in three South African coastal metropolitans using remotely sensed data. Southern African Geographical Journal, 2017, 99, 52-67.	0.9	17
149	Characterizing the spatio-temporal variations of C3 and C4 dominated grasslands aboveground biomass in the Drakensberg, South Africa. International Journal of Applied Earth Observation and Geoinformation, 2018, 68, 51-60.	1.4	17
150	Multispectral mapping of key grassland nutrients in KwaZulu-Natal, South Africa. Journal of Spatial Science, 2018, 63, 155-172.	1.0	17
151	Modelling soil organic carbon stock distribution across different land-uses in South Africa: A remote sensing and deep learning approach. ISPRS Journal of Photogrammetry and Remote Sensing, 2022, 188, 351-362.	4.9	17
152	Detecting the severity of woodwasp, Sirex noctilio, infestation in a pine plantation in KwaZulu-Natal, South Africa, using texture measures calculated from high spatial resolution imagery. African Entomology, 2008, 16, 263-275.	0.6	16
153	Capability of models to predict leaf N and P across four seasons for six sub-tropical forest evergreen trees. ISPRS Journal of Photogrammetry and Remote Sensing, 2015, 101, 209-220.	4.9	16
154	Evaluating the potential of freely available multispectral remotely sensed imagery in mapping American bramble ( <i>Rubus cuneifolius</i> ). Southern African Geographical Journal, 2018, 100, 291-307.	0.9	16
155	Geospatial assessment of soil erosion vulnerability in the upper uMgeni catchment in KwaZulu Natal, South Africa. Physics and Chemistry of the Earth, 2019, 112, 50-57.	1.2	16
156	Improving the classification of six evergreen subtropical tree species with multi-season data from leaf spectra simulated to WorldView-2 and RapidEye. International Journal of Remote Sensing, 2017, 38, 4804-4830.	1.3	16
157	Phenology-based discrimination of maize (Zea mays L.) varieties using multitemporal hyperspectral data. Journal of Applied Remote Sensing, 2019, 13, 1.	0.6	16
158	The Utility of Sentinel-2 Spectral Data in Quantifying Above-Ground Carbon Stock in an Urban Reforested Landscape. Remote Sensing, 2021, 13, 4281.	1.8	16
159	Veld fire reporting and mapping techniques in the Kruger National Park, South Africa, from 1941 to 2011. African Journal of Range and Forage Science, 2012, 29, 63-73.	0.6	15
160	Identifying relevant hyperspectral bands using Boruta: a temporal analysis of water hyacinth biocontrol. Journal of Applied Remote Sensing, 2016, 10, 042002.	0.6	15
161	Use of Landsat series data to analyse the spatial and temporal variations of land degradation in a dispersive soil environment: A case of King Sabata Dalindyebo local municipality in the Eastern Cape Province, South Africa. Physics and Chemistry of the Earth, 2017, 100, 112-120.	1.2	15
162	Stand-volume estimation from multi-source data for coppiced and high forest Eucalyptus spp. silvicultural systems in KwaZulu-Natal, South Africa. ISPRS Journal of Photogrammetry and Remote Sensing, 2017, 132, 162-169.	4.9	15

#	Article	IF	CITATIONS
163	Outdoor thermal discomfort analysis in Harare, Zimbabwe in Southern Africa. Southern African Geographical Journal, 2018, 100, 162-179.	0.9	15
164	Modelling potential distribution of bramble (rubus cuneifolius) using topographic, bioclimatic and remotely sensed data in the KwaZulu-Natal Drakensberg, South Africa. Applied Geography, 2018, 99, 54-62.	1.7	15
165	Using local and indigenous knowledge in selecting indicators for mapping flood vulnerability in informal settlement contexts. International Journal of Disaster Risk Reduction, 2022, 71, 102836.	1.8	15
166	Estimation of Maize Foliar Temperature and Stomatal Conductance as Indicators of Water Stress Based on Optical and Thermal Imagery Acquired Using an Unmanned Aerial Vehicle (UAV) Platform. Drones, 2022, 6, 169.	2.7	15
167	Integrating remote sensing and geostatistics to estimate woody vegetation in an African savanna. Journal of Spatial Science, 2013, 58, 305-322.	1.0	14
168	Implications of land use transitions on soil nitrogen in dynamic landscapes in Tanzania. Land Use Policy, 2017, 64, 95-100.	2.5	14
169	Assessing the potential of Sentinel-2 MSI sensor in detecting and mapping the spatial distribution of gullies in a communal grazing landscape. Physics and Chemistry of the Earth, 2019, 112, 66-74.	1.2	14
170	Investigating the Relationship between Tree Species Diversity and Landsat-8 Spectral Heterogeneity across Multiple Phenological Stages. Remote Sensing, 2021, 13, 2467.	1.8	14
171	A systematic review on the use of remote sensing technologies in quantifying grasslands ecosystem services. GIScience and Remote Sensing, 2022, 59, 1000-1025.	2.4	14
172	Evaluating the influence of the Red Edge band from RapidEye sensor in quantifying leaf area index for hydrological applications specifically focussing on plant canopy interception. Physics and Chemistry of the Earth, 2017, 100, 73-80.	1.2	13
173	Remote sensing of key grassland nutrients using hyperspectral techniques in KwaZulu-Natal, South Africa. Journal of Applied Remote Sensing, 2017, 11, 036005.	0.6	13
174	Detecting and mapping Gonipterus scutellatus induced vegetation defoliation using WorldView-2 pan-sharpened image texture combinations and an artificial neural network. Journal of Applied Remote Sensing, 2019, 13, 1.	0.6	13
175	Detecting and mapping levels of <i>Gonipterus scutellatus</i> -induced vegetation defoliation and leaf area index using spatially optimized vegetation indices. Geocarto International, 2018, 33, 277-292.	1.7	12
176	Deep learning approaches in remote sensing of soil organic carbon: a review of utility, challenges, and prospects. Environmental Monitoring and Assessment, 2021, 193, 802.	1.3	12
177	The potential of remote sensing technology for the detection and mapping ofThaumastocoris peregrinusin plantation forests. Southern Forests, 2011, 73, 23-31.	0.2	11
178	Predicting water stress induced by <i>Thaumastocoris peregrinus</i> infestations in plantation forests using field spectroscopy and neural networks. Journal of Spatial Science, 2014, 59, 79-90.	1.0	11
179	Varietal discrimination of common dry bean (Phaseolus vulgarisL.) grown under different watering regimes using multitemporal hyperspectral data. Journal of Applied Remote Sensing, 2015, 9, 096050.	0.6	11
180	Potential of interval partial least square regression in estimating leaf area index. South African Journal of Science, 2017, 113, 9.	0.3	11

#	Article	IF	CITATIONS
181	Determining Optimal New Generation Satellite Derived Metrics for Accurate C3 and C4 Grass Species Aboveground Biomass Estimation in South Africa. Remote Sensing, 2018, 10, 564.	1.8	11
182	Modelling <i>Parthenium hysterophorus</i> invasion in KwaZulu-Natal province using remotely sensed data and environmental variables. Geocarto International, 2020, 35, 1450-1465.	1.7	11
183	Mapping the Eucalyptus spp woodlots in communal areas of Southern Africa using Sentinel-2 Multi-Spectral Imager data for hydrological applications. Physics and Chemistry of the Earth, 2021, 122, 102999.	1.2	11
184	Estimating urban LST using multiple remotely sensed spectral indices and elevation retrievals. Sustainable Cities and Society, 2022, 78, 103623.	5.1	11
185	The utility of satellite fire product accuracy Information-perspectives and recommendations from the Southern Africa fire network. IEEE Transactions on Geoscience and Remote Sensing, 2006, 44, 1928-1930.	2.7	10
186	Estimating aboveground net primary productivity of reforested trees in an urban landscape using biophysical variables and remotely sensed data. Science of the Total Environment, 2022, 802, 149958.	3.9	10
187	Determining the Influence of Long Term Urban Growth on Surface Urban Heat Islands Using Local Climate Zones and Intensity Analysis Techniques. Remote Sensing, 2022, 14, 2060.	1.8	10
188	Variation in foliar water content and hyperspectral reflectance ofPinus patulatrees infested bySirex noctilio. Southern Forests, 2010, 72, 1-7.	0.2	9
189	Evaluating the Applications of the Near-Infrared Region in Mapping Foliar N in the Miombo Woodlands. Remote Sensing, 2018, 10, 505.	1.8	9
190	Landscape Scale land degradation mapping in the semi-arid areas of the Save catchment, Zimbabwe. Southern African Geographical Journal, 2021, 103, 183-203.	0.9	9
191	Estimation of high density wetland biomass: combining regression model with vegetation index developed from Worldview-2 imagery. Proceedings of SPIE, 2012, , .	0.8	8
192	Scenario-based approach in dealing with climate change impacts in Central Tanzania. Futures, 2017, 85, 30-41.	1.4	8
193	Assessing the utility of topographic variables in predicting structural complexity of tree stands in a reforested urban landscape. Urban Forestry and Urban Greening, 2018, 31, 120-129.	2.3	8
194	The Impact of Simulated Spectral Noise on Random Forest and Oblique Random Forest Classification Performance. Journal of Spectroscopy, 2018, 2018, 1-8.	0.6	8
195	Detection and mapping of maize streak virus using RapidEye satellite imagery. Geocarto International, 2019, 34, 856-866.	1.7	8
196	Estimating soil organic carbon stocks under commercial forestry using topo-climate variables in KwaZulu-Natal, South Africa. South African Journal of Science, 2020, 116, .	0.3	8
197	Fire danger assessment using geospatial modelling in Mekong delta, Vietnam: Effects on wetland resources. Remote Sensing Applications: Society and Environment, 2021, 21, 100456.	0.8	8
198	Progress in Remote Sensing of Grass Senescence: A Review on the Challenges and Opportunities. IEEE Journal of Selected Topics in Applied Earth Observations and Remote Sensing, 2021, 14, 7714-7723.	2.3	8

#	Article	IF	CITATIONS
199	Rearing Rabbits Over Earthen Fish Ponds in Rwanda: Effects on Water and Sediment Quality, Growth, and Production of Nile Tilapia <i>Oreochromis niloticus</i> . Journal of Applied Aquaculture, 2012, 24, 170-181.	0.7	7
200	Evaluation of potential indicators for payment of environmental services on the impact of rehabilitation of degraded rangeland sites. African Journal of Agricultural Research Vol Pp, 2013, 8, 1290-1299.	0.2	7
201	Assessment of the Contribution of WorldView-2 Strategically Positioned Bands in Bracken fern ( <i>Pteridium aquilinum (L.) Kuhn</i> ) Mapping. South African Journal of Geomatics, 2014, 3, 210.	0.1	7
202	Land Use Land Cover Change in the fringe of eThekwini Municipality: Implications for urban green spaces using remote sensing. South African Journal of Geomatics, 2014, 3, 145.	0.1	7
203	Optimizing the spatial resolution of WorldView-2 imagery for discriminating forest vegetation at subspecies level in KwaZulu-Natal, South Africa. Geocarto International, 2016, 31, 870-880.	1.7	7
204	Including shaded leaves in a sample affects the accuracy of remotely estimating foliar nitrogen. GIScience and Remote Sensing, 2019, 56, 1114-1127.	2.4	7
205	The Utility of the Upcoming HyspIRI's Simulated Spectral Settings in Detecting Maize Gray Leafy Spot in Relation to Sentinel-2 MSI, VENAµS, and Landsat 8 OLI Sensors. Agronomy, 2019, 9, 846.	1.3	7
206	Distribution of Parthenium hysterophoru L. with variation in rainfall using multi-year SPOT data and random forest classification. Remote Sensing Applications: Society and Environment, 2019, 13, 215-223.	0.8	7
207	Analysing fragmentation in vulnerable biodiversity hotspots in Tanzania from 1975 to 2012 using remote sensing and fragstats. Nature Conservation, 0, 16, 19-37.	0.0	7
208	A spatial and temporal assessment of fire regimes on different vegetation types using MODIS burnt area products. Bothalia, 2016, 46, .	0.2	7
209	Spectral discrimination of increaser species as an indicator of rangeland degradation using field spectrometry. Journal of Spatial Science, 2013, 58, 101-117.	1.0	6
210	An Analysis of Ecosystem Vulnerability and Management Interventions in the Morogoro Region Landscapes, Tanzania. Tropical Conservation Science, 2015, 8, 662-680.	0.6	6
211	Predicting medicinal phytochemicals of <i>Moringa oleifera</i> using hyperspectral reflectance of tree canopies. International Journal of Remote Sensing, 2021, 42, 3955-3980.	1.3	6
212	Mapping foliar N in miombo woodlands using sentinel-2 derived chlorophyll and structural indices. Journal of Applied Remote Sensing, 2018, 12, 1.	0.6	6
213	Landscape fragmentation in coffee agroecological subzones in central Kenya: a multiscale remote sensing approach. Journal of Applied Remote Sensing, 2020, 14, .	0.6	6
214	Assessing habitat fragmentation of the KwaZulu-Natal Sandstone Sourveld, a threatened ecosystem. Bothalia, 2016, 46, .	0.2	6
215	The use of multisource spatial data for determining the proliferation of stingless bees in Kenya. GIScience and Remote Sensing, 2022, 59, 648-669.	2.4	6
216	Determining the onset of autumn grass senescence in subtropical sour-veld grasslands using remote sensing proxies and the breakpoint approach. Ecological Informatics, 2022, 69, 101651.	2.3	6

#	Article	IF	CITATIONS
217	Geostatistical Analysis of Quality Protein Maize Outcrossing with Pollen from Adjacent Normal Endosperm Maize Varieties. Crop Science, 2012, 52, 1235-1245.	0.8	5
218	Classifying increaser species as an indicator of different levels of rangeland degradation using WorldView-2 imagery. Journal of Applied Remote Sensing, 2012, 6, 063558-1.	0.6	5
219	Exploring the utility of the additional WorldView-2 bands and support vector machines in mapping land use/land cover in a fragmented ecosystem, South Africa. South African Journal of Geomatics, 2015, 4, 414.	0.1	5
220	Predicting the distribution of C3 ( <i>Festuca</i> spp.) grass species using topographic variables and binary logistic regression model. Geocarto International, 2018, 33, 489-504.	1.7	5
221	Optimal season for discriminating C3 and C4 grass functional types using multi-date Sentinel 2 data. GIScience and Remote Sensing, 2020, 57, 127-139.	2.4	5
222	Quantifying grass productivity using remotely sensed data: an assessment of grassland restoration benefits. African Journal of Range and Forage Science, 2020, 37, 247-256.	0.6	5
223	Rainfall Trend and Its Relationship with Normalized Difference Vegetation Index in a Restored Semi-Arid Wetland of South Africa. Sustainability, 2020, 12, 8919.	1.6	5
224	Mapping the spatial distribution of the yellowwood tree (Podocarpus henkelii) in the Weza-Ngele forest using the newly launched Sentinel-2 multispectral imager data. Southern African Geographical Journal, 2021, 103, 204-222.	0.9	5
225	Understanding participatory GIS application in rangeland use planning: a review of PGIS practice in Africa. Journal of Land Use Science, 2021, 16, 174-187.	1.0	5
226	Functional land cover scale for three insect pests with contrasting dispersal strategies in a fragmented coffee-based landscape in Central Kenya. Agriculture, Ecosystems and Environment, 2021, 319, 107558.	2.5	5
227	Spectrometric proximally sensed data for estimating chlorophyll content of grasslands treated with complex fertilizer combinations. Journal of Applied Remote Sensing, 2020, 14, 1.	0.6	5
228	Determining the Capability of the Tree-Based Pipeline Optimization Tool (TPOT) in Mapping Parthenium Weed Using Multi-Date Sentinel-2 Image Data. Remote Sensing, 2022, 14, 1687.	1.8	5
229	Merging Double Sampling with Remote Sensing for a Rapid Estimation of Fuelwood. Geocarto International, 2004, 19, 49-55.	1.7	4
230	Field spectrometry of papyrus vegetation (Cyperus papyrus L.) in swamp wetlands of St Lucia, South Africa. , 2009, , .		4
231	Measuring quality performance of cadastral survey and deeds registration work processes. Land Use Policy, 2011, 28, 38-46.	2.5	4
232	Optimum rabbit density over fish ponds to optimise Nile tilapia production in an integrated rabbit–fish system in Rwanda. African Journal of Aquatic Science, 2012, 37, 165-174.	0.5	4
233	Remote sensing bio-control damage on aquatic invasive alien plant species. South African Journal of Geomatics, 2015, 4, 464.	0.1	4
234	A Hybrid Feature Method for Handling Redundant Features in a Sentinel-2 Multidate Image for Mapping Parthenium Weed. IEEE Journal of Selected Topics in Applied Earth Observations and Remote Sensing, 2020, 13, 3644-3655.	2.3	4

ONISIMO MUTANGA

#	Article	IF	CITATIONS
235	Testing the utility of multivariate techniques in mapping commercial forest species using freely available Landsat 8 Operational Land Imager (OLI). Journal of Forest Research, 2020, 25, 354-357.	0.7	4
236	Optimal window period for mapping Parthenium weed in South Africa, using high temporal resolution imagery and the ExtraTrees classifier. Biological Invasions, 2021, 23, 2881-2892.	1.2	4
237	Detecting and mapping the spatial distribution of Chromoleana odorata invasions in communal areas of South Africa using Sentinel-2 multispectral remotely sensed data. Physics and Chemistry of the Earth, 2022, 126, 103081.	1.2	4
238	Mapping rangeland ecosystems vulnerability to <i>Lantana camara</i> invasion in semiâ€arid savannahs in South Africa. African Journal of Ecology, 2022, 60, 658-667.	0.4	4
239	Pansharpened landsat 8 thermal-infrared data for improved Land Surface Temperature characterization in a heterogeneous urban landscape. Remote Sensing Applications: Society and Environment, 2022, 26, 100728.	0.8	4
240	Monitoring the Spatio-Temporal Variations of C3/C4 Grass Species Using Multispectral Satellite Data. , 2018, , .		3
241	Discrimination of Tomato Plants (Solanum lycopersicum) Grown under Anaerobic Baffled Reactor Effluent, Nitrified Urine Concentrates and Commercial Hydroponic Fertilizer Regimes Using Simulated Sensor Spectral Settings. Agronomy, 2019, 9, 373.	1.3	3
242	Assessing edge effect on the spatial distribution of selected forest biochemical properties derived using the Worldview data in Dukuduku forests, South Africa. African Journal of Ecology, 2019, 57, 314-326.	0.4	3
243	Remote sensing equivalent water thickness of grass treated with different fertiliser regimes using resample HysplRI and EnMAP data. Physics and Chemistry of the Earth, 2019, 112, 246-254.	1.2	3
244	Automated classification of a tropical landscape infested by Parthenium weed (Parthenium) Tj ETQq0 0 0 rgBT /0	Dverlock 1 1.3	0 Tf 50 382 T
245	Improving the unsupervised mapping of riparian bugweed in commercial forest plantations using hyperspectral data and LiDAR. Geocarto International, 2021, 36, 465-480.	1.7	3
246	Estimating leaf area index of the Yellowwood tree ( <i>Podocarpus spp.)</i> in an indigenous Southern African Forest, using Sentinel 2 Multispectral Instrument data and the Random Forest regression ensemble. Geocarto International, 2022, 37, 6953-6974.	1.7	3
247	Quantitative remote sensing of forest ecosystem services in sub-Saharan Africa's urban landscapes: a review. Environmental Monitoring and Assessment, 2022, 194, 242.	1.3	3
248	A comparison of selected machine learning classifiers in mapping a South African heterogeneous coastal zone: Testing the utility of an object-based classification with WorldView-2 imagery. , 2012, , .		2
249	Estimating canopy nitrogen concentration across C3 and C4 grasslands using WorldView-2 multispectral data and the random forest algorithm. , 2013, , .		2
250	Integrating remote sensing and conventional grazing/browsing models for modelling carrying capacity in southern African rangelands. , 2014, , .		2
251	Development of census output areas with AZTool in South Africa. South African Journal of Science, 2016, 112, 7.	0.3	2
252	Modelling Leaf Chlorophyll Content in Coffee (Coffea Arabica) Plantations Using Sentinel 2 Msi Data. , 2018, , .		2

ONISIMO MUTANGA

#	Article	IF	CITATIONS
253	Testing the spectral resolutions of the new multispectral sensors for detecting <i>Phaeosphaeria</i> leaf spot (PLS) infestations in maize crop. South African Journal of Geomatics, 2018, 7, 1.	0.1	2
254	Remote estimation of nitrogen is more accurate at the start of the growing season when compared with end of the growing season in miombo woodlands. Remote Sensing Applications: Society and Environment, 2020, 17, 100285.	0.8	2
255	Mapping the spatial distribution of <i>Lantana camara</i> using high-resolution SPOT 6 data, in Mpumalanga communal areas, South Africa. Transactions of the Royal Society of South Africa, 2020, 75, 239-244.	0.8	2
256	Spatially optimizing vegetation indices integrated with sparse partial least squares regression to detect and map the effects of Gonipterus scutellatus on the chlorophyll content of eucalyptus plantations. International Journal of Remote Sensing, 2020, 41, 6444-6459.	1.3	2
257	Characterizing bracken fern phenological cycle using time series data derived from Sentinel-2 satellite sensor. PLoS ONE, 2021, 16, e0257196.	1.1	2
258	Using participatory GIS and collaborative management approaches to enhance local actors' participation in rangeland management: the case of Vulindlela, South Africa. Journal of Environmental Planning and Management, 2023, 66, 1189-1208.	2.4	2
259	Understanding Growth-Induced Trends in Local Climate Zones, Land Surface Temperature, and Extreme Temperature Events in a Rapidly Growing City: A Case of Bulawayo Metropolitan City in Zimbabwe. Frontiers in Environmental Science, 0, 10, .	1.5	2
260	Unsupervised anomaly weed detection in riparian forest areas using hyperspectral data and LiDAR. , 2016, , .		1
261	Determining the optimal phenological stage for predicting common dry bean (Phaseolus vulgaris) yield using field spectroscopy. South African Journal of Plant and Soil, 2017, 34, 379-388.	0.4	1
262	Predicting Urban Growth and Implication on Urban Thermal Characteristics in Harare, Zimbabwe. , 2018, , .		1
263	A Comparison of Regression Tree Approaches to Modelling the Efficacy of Water Hyacinth Biocontrol Using Multitemporal Spectral Datasets. Journal of Spectroscopy, 2018, 2018, 1-11.	0.6	1
264	Optimising Sentinel-2 MSI spatial resolution for estimating foliar nitrogen concentration in miombo woodlands. Journal of Spatial Science, 2023, 68, 107-121.	1.0	1
265	Detecting and mapping invasive Parthenium hysterophorus L. along the northern coastal belt of KwaZulu-Natal, South Africa using image texture. Scientific African, 2021, 13, e00966.	0.7	1
266	The Utility of Sentinel-2 MSI Data to Estimate Wetland Vegetation Leaf Area Index in Natural and Rehabilitated Wetlands. Geographies, 2021, 1, 178-191.	0.6	1
267	Effects of different building blocks designs on the statistical characteristics of Automated Zone-design Tool output areas. South African Journal of Geomatics, 2017, 6, 155.	0.1	0
268	Suitability of resampled multispectral datasets for mapping flowering plants in the Kenyan savannah. PLoS ONE, 2020, 15, e0232313.	1.1	0
269	Leveraging of hyperspectral remote sensing on estimating biomass yield of Moringa oleifera Lam. medicinal plant. South African Journal of Botany, 2021, 140, 37-49.	1.2	0
270	Discriminating tropical grasses grown under different nitrogen fertilizer regimes in KwaZulu-Natal, South Africa. , 2020, , 147-163.		0

#	Article	IF	CITATIONS
271	Testing the value of freely available Landsat 8 Operational Land Imager (OLI) and OLI pan-sharpened imagery in discriminating commercial forest species. Southern African Geographical Journal, 2021, 103, 501-518.	0.9	0
272	Synergistic potential of dual-polarized synthetic aperture radar and multispectral optical imagery for invasive alien species detection and mapping. Journal of Applied Remote Sensing, 2020, 14, 1.	0.6	0
273	Mapping leaf area index of the Yellowwood tree species in an Afromontane mistbelt forest of southern Africa using topographic variables. Remote Sensing Applications: Society and Environment, 2022, 27, 100778.	0.8	0